Nonlinear Anal. RWA 78 (2024) 104097

Contents lists available at ScienceDirect

Nonlinear Analysis: Real World Applications

journal homepage: www.elsevier.com/locate/nonrwa

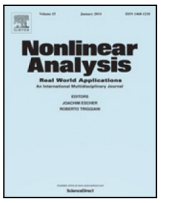

Dynamics of a mathematical model of virus spreading incorporating the effect of a vaccine

Aytül Gökçe [a,1], Burcu Gürbüz [b,*,1], Alan D. Rendall [b,1]

[a] Ordu University, Faculty of Science and Letters, Department of Mathematics, 52200, Ordu, Turkey
[b] Institut für Mathematik, Johannes Gutenberg-Universität, Staudingerweg 9, 55099, Mainz, Germany

ARTICLE INFO

Keywords:
Epidemic model
COVID-19
Backward bifurcation
Local stability

ABSTRACT

The COVID-19 pandemic led to widespread interest in epidemiological models. In this context the role of vaccination in influencing the spreading of the disease is of particular interest. There has also been a lot of debate on the role of non-pharmaceutical interventions such as the disinfection of surfaces. We investigate a mathematical model for the spread of a disease which includes both imperfect vaccination and infection due to virus in the environment. The latter is studied with the help of two phenomenological models for the force of infection. In one of these models we find that backward bifurcations take place so that for some parameter values an endemic steady state exists although the basic reproduction ratio $\mathcal{R}_0$ is less than one. We also prove that in that case there can exist more than one endemic steady state. In the other model all generic transcritical bifurcations are forward bifurcations so that these effects cannot occur. Thus we see that the occurrence of backward bifurcations, which can be important for disease control strategies, is dependent on the details of the function describing the force of infection. By means of simulations the predictions of this model are compared with data for COVID-19 from Turkey. A sensitivity analysis is also carried out.

1. Introduction

Since the beginning of epidemiology mathematical models have played a central role. This can be seen in the groundbreaking work of Ronald Ross and Hilda Hudson on the eradication of malaria [1–3]. In that work the authors identified a threshold for the persistence of a disease which can be seen as the ancestor of the basic reproduction ratio $\mathcal{R}_0$ which is so important in epidemiology today. The COVID-19 epidemic caused a surge of work where epidemiological models were defined, simulated and subjected to rigorous mathematical analysis. Due to the urgency of the situation this development took place in a rather disorganized way. Now it is time to consolidate and extend the things learned at that time so as to be prepared as well as possible for future epidemics.

In this paper we study a model for the spread of an infectious disease in a human population which includes an imperfect vaccination and takes into account infections due to virus particles in the environment. In particular we are thinking of fomites, objects in the environment which are contaminated with virus and which are not humans or animals. Here we may think of the contamination by hands touching doorknobs [4] or infections spreading in hospitals [5]. The question of how important this route of infection is for COVID-19 has been a subject of much discussion. The consensus appears to be that it is of secondary importance but this may be different for other diseases [6,7].

* Corresponding author.
E-mail addresses: aytulgokce@odu.edu.tr (A. Gökçe), burcu.gurbuz@uni-mainz.de (B. Gürbüz), rendall@uni-mainz.de (A.D. Rendall).
[1] All authors contributed equally to this work.

https://doi.org/10.1016/j.nonrwa.2024.104097
Received 5 October 2023; Received in revised form 19 February 2024; Accepted 21 February 2024
Available online 24 February 2024

In Section 2 we define the model which is of central interest in this paper and establish some basic properties of its solutions. The model contains a response function which describes how the concentration of virus in the environment affects the rate of infection by this route. This function depends on an integer $n \geq 1$. The motivation for the choice of this function is also discussed. In Section 2.1 it is shown that this model has a unique disease-free steady state (Lemma 1) and the stability of that state is determined using the next generation matrix. The basic reproduction ratio $\mathcal{R}_0$ is computed for this model and it is shown to be a decreasing function of the vaccination rate. The existence of backward bifurcations is analysed using the method of van den Driessche and Watmough [8]. It is proved that generic backward bifurcations occur in the case $n = 2$ but not otherwise (Theorem 1). In particular they do not occur in the case $n = 1$, where the function describing the force of infection is one which had previously been considered in the literature [9]. Note that an existing model for imperfect vaccination [10] also exhibits no backward bifurcations. A backward bifurcation is often accompanied by the presence of more than one positive steady state for given values of the parameters (cf. [11]). In many cases of backward bifurcations simulations show not only that for a certain choice of parameters positive steady states exist for $\mathcal{R}_0 < 1$ but also that two positive steady states can occur. It is proved in Section 4 that there are parameters for which our model with $n = 2$ exhibits the latter behaviour. In Section 5 it is shown that solutions of the model can be fitted to COVID-19 data from Turkey. Section 6 carries out a sensitivity analysis of the model.

2. The model

The model considered in what follows is a generalization of one introduced in [10] to study the effects of vaccination against SARS and is given by the following equations:

$$\frac{dS}{dt} = \Lambda - \beta SI - \sigma S + (1-\lambda)t'V - \alpha_1 S g(C,\kappa) - \mu S, \tag{1}$$

$$\frac{dE}{dt} = \beta SI + \epsilon IV - \xi E - \mu E + \alpha_1 S g(C,\kappa) + \alpha_2 V g(C,\kappa), \tag{2}$$

$$\frac{dI}{dt} = \xi E - \delta I - dI - \mu I, \tag{3}$$

$$\frac{dV}{dt} = \sigma S - \epsilon IV - (t' + \mu)V - \alpha_2 V g(C,\kappa), \tag{4}$$

$$\frac{dR}{dt} = \delta I - \mu R + \lambda t' V, \tag{5}$$

$$\frac{dC}{dt} = \varphi I - \omega C, \tag{6}$$

where

$$g(C,\kappa) = \frac{C^n}{C^n + \kappa}.$$

The meaning of the parameters in this model is described in Table 1. The model of [10] was called an SVEIR model after the names of its five unknowns S, V, E, I and R. These are the numbers of susceptible, vaccinated, exposed, infectious and recovered individuals, respectively. We augment this by an additional variable C representing the concentration of the virus in the environment. In both models the vaccination is imperfect but the imperfection is of a different kind. Correspondingly the class V has a different interpretation in the two models. In [10] the class V consists of individuals who have been vaccinated at some time. The effect of the vaccination is to lower the rate at which they get infected compared to unvaccinated individuals. In the model (1)–(6) the class V consists of individuals who have received a vaccination but where the vaccination has not yet had time to become fully effective. After that time either the vaccination provides complete protection or it has not been effective and the individual returns to the susceptible class. For biological reasons the inequalities $\epsilon \leq \beta$ and $\alpha_2 \leq \alpha_1$ are assumed, which means that vaccinated individuals are no more likely to be infected than unvaccinated individuals, either by infected individuals or by contact with their surroundings.

Mathematically the model of [10], up to a different notation, can be obtained from our model by setting $t' = \alpha_1 = \alpha_2 = 0$ and discarding the equation for S. This is possible since when the parameters just listed are zero the equations for the first five variables to not depend on S. In the model (1)–(6) the imperfection of the vaccination is expressed as follows. Individuals leave the vaccinated state at rate t', the vaccination having been successful with probability λ. This way of modelling an imperfect vaccination was previously used in [12]. The other additional effect taken account of in (1)–(6) is related to infection by virus in the environment. It is expressed by the terms containing the factors α_1 and α_2 relating to the unvaccinated and vaccinated individuals, respectively. This type of effect was included in a model of [9]. In that paper the function g written above with $n = 1$ was used as a phenomenological description of the rate of infection in this process. It would be possible to generalize the model by choosing different values of the parameter n in Eqs. (1), (2) and (4), which would implement a difference in the process of infection in the groups E and V. Since, however, we do not know any reason why a difference of this kind should exist we have not analysed this generalization.

It is worth taking some time to discuss the status of this type of phenomenological description. It is used in defining response functions in various parts of biology. In biochemistry the case $n = 1$ is called a Michaelis–Menten function while the case $n \geq 2$ is called a Hill function. In predator–prey models in ecology the case $n = 1$ is called Holling type II while the case $n \geq 2$ is called Holling type III. Holling type I denotes a linear response function, usually with a cut-off. A general discussion of response functions in epidemiology is given in Chapter 10 of the book of Diekmann and Heesterbeek [13], whereby the authors make clear from the beginning that they do not claim to give a definitive answer to the questions they are raising.

Suppose that there is a source of infection with intensity Z and a population S of susceptibles. Let $F(Z,S)$ be the rate of infection. In principle this could be any function. Let us suppose that F depends linearly on S but initially allow its dependence on Z to be

Table 1
Parameters used in the model.

Parameters	Biological meaning
Λ	Recruitment rate
β	Effective contact rate with βS new susceptible individuals per unit time
α_1	Transmission ratio of the virus from the environment to susceptible individuals that enter the exposed class
α_2	Transmission ratio of the virus from the environment to vaccinated individuals (not fully immunized) that may enter the exposed class
ϵ	The rate at which a vaccinated individual (not fully immunized) becomes exposed after being in contact with an infected individual
δ	The rate of recovered individuals
μ	Natural mortality rate
ξ	Rate of development of clinical symptoms
d	Disease induced fatality rate
σ	Vaccination rate of susceptible individuals (the first shot)
φ	The virus exposure rate
λ	The efficiency of the vaccine
t'^{-1}	The mean amount of time that is spent in the vaccinated class before developing an immune response and moving to the recovery class.
ω	The rate of decay in the virus density

arbitrary. Thus $F(Z,S) = Sf(Z)$ for some function f. What properties should the function f have? It should be positive for Z positive and zero for $Z = 0$. It should be non-decreasing. It is reasonable to assume that it is bounded. The simplest type of function satisfying these requirements is one of the form $f(Z) = \frac{aZ}{Z+b}$. Another situation in which a response function is of relevance is the predation rate in a predator–prey model. There the analogue of I is the density of predators while the analogue of Z is the density of prey. In that case a function of the form just considered is called Holling type II. In that context Holling type I is a function which is linear up to a threshold value and then constant. Holling type III corresponds to Z being replaced by Z^p. This argument for introducing a function f of this form is purely phenomenological. Holling had a mechanistic argument to motivate his type II function. There have also been attempts to motivate the type III function by mechanistic considerations (cf. [14,15]). We are not aware that this has been done in epidemiology. The function corresponding to Holling type II was introduced to epidemiological models by Dietz [16], without a mechanistic background. Holling's mechanistic approach does not apply to epidemiological models. Diekmann and Heesterbeek [13] discuss mechanistic approaches to the Holling type II function in epidemiology. In fact in a model case they derive something which is not a rational function. We have not found a paper where the Holling type III function is used in epidemiology.

The right hand sides of Eqs. (1)–(6) are smooth and hence for any initial values at a given time they have a unique solution on some time interval. Because of the interpretation of the unknowns we are interested in solutions which are non-negative at all times. This is true provided the initial data are non-negative (cf. [17], Lemma 1). Let $N(t) = S(t) + E(t) + I(t) + V(t) + R(t)$. Then

$$\frac{\mathrm{d}N}{\mathrm{d}t} = \Lambda - \mu N - dI \leq \Lambda - \mu N. \tag{7}$$

This implies that N remains bounded on any finite time interval. Hence on such an interval all variables other than C are bounded. It then follows from (6) that C is also bounded. As a consequence the solutions exist globally in the future. Using the differential inequality for N again shows that

$$\limsup_{t\to\infty} N(t) \leq \frac{\Lambda}{\mu}. \tag{8}$$

It then follows from (6) that $\limsup_{t\to\infty} C(t) \leq \frac{\Lambda\varphi}{\mu\omega}$.

2.1. The disease-free steady state

Consider a boundary steady state $(S^*, E^*, I^*, V^*, R^*, C^*)$ of the system (1)–(6), i.e. a time-independent solution for which at least one of the unknowns is zero.

Lemma 1. *The model (1)–(6) has a unique boundary steady state for any positive values of the parameters and it is of the form* $(S^*, 0, 0, V^*, R^*, 0)$.

Proof. Let $(S^*, E^*, I^*, V^*, R^*, C^*)$ be a boundary steady state. If $S^* = 0$ then (1) gives a contradiction and so $S^* \neq 0$. If $V^* = 0$ then (4) implies that $S^* = 0$. Hence in fact $V^* \neq 0$. If $R^* = 0$ then (6) implies that $V^* = 0$. Hence in fact $R^* \neq 0$. It follows from the other three equations that for a steady state the equations $E^* = 0$, $I^* = 0$ and $C^* = 0$ are all equivalent to each other. Hence any boundary steady state is of the form $(S^*, 0, 0, V^*, R^*, 0)$. In this case the steady state equations are equivalent to the system

$$\begin{aligned} \Lambda - \sigma S^* + (1-\lambda)t'V^* - \mu S^* &= 0, \\ \sigma S^* - (t' + \mu)V^* &= 0, \end{aligned} \tag{9}$$

Table 2
Biologically meaningful parameters used in Fig. 1.

Parameters	Value ($n = 1$)	Unit	Source
Λ	3032	day^{-1}	Assumed based on [10,18,19]
β	0.15×10^{-8}	day^{-1}	Assumed based on [10]
μ	3.653×10^{-5}	day^{-1}	Assumed based on [9,10]
ϵ	0.15×10^{-8}	day^{-1}	Assumed based on [10,12]
t'	1/120	day^{-1}	Assumed based on [12]
λ	0.8	day^{-1}	Assumed based on [12,20,21]
d	0.02	day^{-1}	Assumed based on [9,22]
α_1	0.01	day^{-1}	Assumed
α_2	0.01	day^{-1}	Assumed
ω	4	day^{-1}	[9]
φ	2	day^{-1}	[9]
κ	20 000	copies/day	Assumed based on [9]
ξ	0.125	day^{-1}	[10]
δ	0.06	day^{-1}	Assumed based on [10,12]
σ	0.01	day^{-1}	[12]

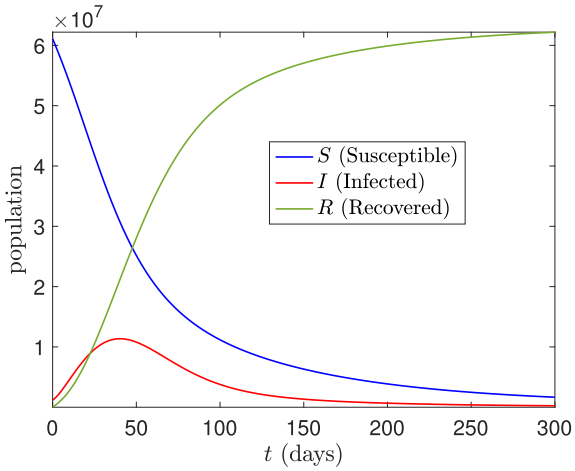

Fig. 1. Simulation result of the model (1)–(6) with initial data and parameters given in Table 2.

$$-\mu R^* + \lambda t' V^* = 0,$$

and these can be solved to give

$$S^* = \frac{\Lambda(t' + \mu)}{\mu(\sigma + t' + \mu) + \lambda t'\sigma}, \tag{10}$$

$$V^* = \frac{\Lambda\sigma}{\mu(\sigma + t' + \mu) + \lambda t'\sigma}, \tag{11}$$

$$R^* = \frac{\lambda t' \Lambda\sigma}{\mu(\mu(\sigma + t' + \mu) + \lambda t'\sigma)}. \tag{12}$$

Thus there exists a unique boundary steady state of this model whose explicit form is given by (10)–(12). ■

All the variables corresponding to the presence of infection are zero in this state and so we call it the disease-free steady state.

To illustrate how a solution of this model corresponding to an epidemic might look we show the results of a simulation with biologically motivated parameters. Table 2 lists the references which were used either as direct sources or guidelines for the choice of the parameters. Fig. 1 demonstrates the dynamics of populations during an epidemic for 300 days. Susceptible (S), Infected (I) and Recovered (R) populations respectively associated with blue, red and green lines. The initial conditions are chosen as $S_0 = 61098000, V_0 = 18500000, E_0 = 2200000, I_0 = 1200000$ and $R_0 = 2000$ and parameters are given in Table 2. It should be noted that these initial conditions and parameters are only selected for illustrative purposes and may not be epidemiologically realistic.

Here a dramatic increase can be seen in the number of infected individuals until day 45, then a gentle decline appears for the population of infected individuals. As is observed from the graph the number of susceptible individuals slowly decreases to 16000000 and while the number of recovered individuals rises above 62000000 at day 290. The total population is taken as 83 million.

3. Stability of the disease-free steady state

Linearization around the disease-free steady state leads to the Jacobian matrix

$$\mathcal{J} = [J_{ij}]_{6\times 6}\Big|_{E^*}, \text{ for } i,j = 1,2,\dots,6, \tag{13}$$

where $E^* = (S^*, 0, 0, V^*, R^*, 0)$ and

$$\begin{aligned}
&J_{11} = -\sigma-\mu,\ J_{12}=0,\ J_{13}=-\beta S,\ J_{14}=(1-\lambda)t',\ J_{15}=0,\ J_{16}=-\alpha_1 S\delta_{1n}/\kappa,\\
&J_{21}=0,\ J_{22}=-\xi-\mu,\ J_{23}=\epsilon V+\beta S,\ J_{24}=0,\ J_{25}=0,\ J_{26}=(\alpha_1 S+\alpha_2 V)\delta_{1n}/\kappa,\\
&J_{31}=0,\ J_{32}=\xi,\ J_{33}=-(\delta+d+\mu),\ J_{34}=0,\ J_{35}=0,\ J_{36}=0,\\
&J_{41}=\sigma,\ J_{42}=0,\ J_{43}=-\epsilon V,\ J_{44}=-(t'+\mu),\ J_{45}=0,\ J_{46}=-\alpha_2 V\delta_{1n}/\kappa,\\
&J_{51}=0,\ J_{52}=0,\ J_{53}=\delta,\ J_{54}=\lambda t',\ J_{55}=-\mu, J_{56}=0,\\
&J_{61}=0,\ J_{62}=0,\ J_{63}=\varphi,\ J_{64}=0,\ J_{65}=0,\ J_{66}=-\omega.
\end{aligned}$$

Here δ_{1n} is a Kronecker delta. Then we have the matrix

$$\mathcal{J} = \begin{bmatrix}
J_{11} & 0 & J_{13} & J_{14} & 0 & J_{16}\\
0 & J_{22} & J_{23} & 0 & 0 & J_{26}\\
0 & J_{32} & J_{33} & 0 & 0 & 0\\
J_{41} & 0 & J_{43} & J_{44} & 0 & J_{46}\\
0 & 0 & J_{53} & J_{54} & J_{55} & 0\\
0 & 0 & J_{63} & 0 & 0 & J_{66}
\end{bmatrix}$$

It is clear that one of the eigenvalues of the Jacobian is J_{55}. Moreover, removing the fifth row and column and interchanging the second row and column with the fourth leads to a matrix with block diagonal structure. Thus two further eigenvalues of the Jacobian can be obtained as the eigenvalues of the matrix

$$\overline{\mathcal{J}_1} = \begin{bmatrix} J_{11} & J_{14}\\ J_{41} & J_{44}\end{bmatrix}.$$

Now

$$\begin{aligned}
\operatorname{tr}\overline{\mathcal{J}_1} &= J_{11}+J_{44} = -(\sigma+\mu)-(t'+\mu) < 0\\
\det\overline{\mathcal{J}_1} &= (\sigma+\mu)(t'+\mu)-\sigma(1-\lambda)t'\\
&= \mu(\sigma+\mu+t')+\sigma\lambda t' > 0.
\end{aligned}$$

Thus the eigenvalues of $\overline{\mathcal{J}_1}$ have negative real parts. The remaining three eigenvalues of the Jacobian are the eigenvalues of the matrix

$$\overline{\mathcal{J}_2} = \begin{bmatrix} J_{22} & J_{23} & J_{26}\\ J_{32} & J_{33} & 0\\ 0 & J_{63} & J_{66}\end{bmatrix},$$

leading to characteristic polynomial

$$(\ell - J_{22})(\ell - J_{33})(\ell - J_{66}) - J_{23}J_{32}(\ell - J_{66}) - J_{26}J_{32}J_{63} = 0,$$

which can be rewritten as

$$\ell^3 + \mathcal{A}_1\ell^2 + \mathcal{A}_2\ell + \mathcal{A}_3 = 0, \tag{14}$$

where

$$\begin{aligned}
\mathcal{A}_1 &= -J_{22}-J_{33}-J_{66},\\
\mathcal{A}_2 &= J_{22}J_{33}-J_{23}J_{32}+J_{66}(J_{22}+J_{33}),\\
\mathcal{A}_3 &= -J_{22}J_{33}J_{66}\left(1-\frac{J_{32}\left(J_{23}J_{66}-J_{63}J_{26}\right)}{J_{22}J_{33}J_{66}}\right).
\end{aligned} \tag{15}$$

The Routh–Hurwitz criterion says that all roots of the characteristic Eq. (14) have negative real parts if and only if $\mathcal{A}_1 > 0$, $\mathcal{A}_1\mathcal{A}_2 > \mathcal{A}_3$ and $\mathcal{A}_3 > 0$ and if these conditions hold the disease-free steady state is asymptotically stable. It is clear that the first condition holds but it is not so easy to see when the second and third conditions hold. It will later be proved indirectly using the next generation matrix that they hold in this model for all values of the parameters.

3.1. The next generation matrix

In this section, following the ideas presented in [8], the basic reproduction ratio for (1)–(6) is derived using the next generation matrix method. We use the notation of [8]. To apply this method we must choose which of the unknowns represent groups of infected individuals and which terms in the equations represent new infections. In fact we choose E, I and C to be the infected variables and the terms which are non-negative and non-linear in the unknowns to represent new infections. The conditions (A1)-(A5) of [8] are satisfied. Most of these are rather obvious for this model. The only exception is (A5) which holds because the quantities corresponding to J_{23} and J_{26} are zero in the case that new infections are turned off. The matrix $\mathcal{F}$ associated with new infections and the matrix $\mathcal{V}$ containing the remaining expressions are given by

$$\mathcal{F} = \begin{bmatrix} 0 \\ \beta SI + \epsilon VI + (\alpha_1 S + \alpha_2 V) g(C,\kappa) \\ 0 \\ 0 \\ 0 \\ 0 \end{bmatrix},$$

and

$$-\mathcal{V} = \begin{bmatrix} 0 \\ \xi E + \mu E \\ -\xi E + \delta I + dI + \mu I \\ 0 \\ 0 \\ -\varphi I + \omega C \end{bmatrix},$$

$\mathcal{V}_+$ and $\mathcal{V}_-$ are the positive and negative parts of $\mathcal{V}$, respectively. Hence the matrices F and V of [8] are given by

$$F\Big|_{E^*} = \begin{bmatrix} 0 & \beta S^* + \epsilon V^* & \delta_{1n}\left(\alpha_1 S^* + \alpha_2 V^*\right)/\kappa \\ 0 & 0 & 0 \\ 0 & 0 & 0 \end{bmatrix}, \; V\Big|_{E^*} = \begin{bmatrix} \xi+\mu & 0 & 0 \\ -\xi & \delta+d+\mu & 0 \\ 0 & -\varphi & \omega \end{bmatrix},$$

The reproduction ratio $\mathcal{R}_0$ is defined (cf. [8,9]) to be the spectral radius of the matrix given by

$$FV^{-1} = \begin{bmatrix} FV_{11}^{-1} & FV_{12}^{-1} & FV_{13}^{-1} \\ 0 & 0 & 0 \\ 0 & 0 & 0 \end{bmatrix},$$

where

$$FV_{11}^{-1} = \frac{\xi}{(\xi+\mu)(\mu+\delta+d)}\left[\left(\beta + \frac{\delta_{1n}\alpha_1\varphi}{\omega\kappa}\right)S^* + \left(\epsilon + \frac{\delta_{1n}\alpha_2\varphi}{\omega\kappa}\right)V^*\right],$$
$$FV_{12}^{-1} = \frac{1}{(\mu+\delta+d)}\left[\left(\beta + \frac{\delta_{1n}\alpha_1\varphi}{\omega\kappa}\right)S^* + \left(\epsilon + \frac{\delta_{1n}\alpha_2\varphi}{\omega\kappa}\right)V^*\right],$$
$$FV_{13}^{-1} = \frac{\delta_{1n}}{\omega\kappa}\left(\alpha_1 S^* + \alpha_2 V^*\right)$$

The characteristic equation of this matrix is given by

$$\det(FV^{-1} - \Sigma I) = 0.$$

Its roots are the eigenvalues:

$$\Sigma_1 = \frac{\xi}{(\xi+\mu)(\mu+\delta+d)}\left[\left(\beta + \frac{\delta_{1n}\alpha_1\varphi}{\omega\kappa}\right)S^* + \left(\epsilon + \frac{\delta_{1n}\alpha_2\varphi}{\omega\kappa}\right)V^*\right], \tag{16}$$
$$\Sigma_2 = 0, \tag{17}$$
$$\Sigma_3 = 0. \tag{18}$$

Thus the basic reproduction ratio, which is associated with the dominant eigenvalue Σ_1, is

$$\begin{aligned}\mathcal{R}_0 &= \frac{\xi S^*}{(\xi+\mu)(\mu+\delta+d)}\left[\left(\beta + \frac{\delta_{1n}\alpha_1\varphi}{\omega\kappa}\right) + \left(\epsilon + \frac{\delta_{1n}\alpha_2\varphi}{\omega\kappa}\right)\frac{\sigma}{t'+\mu}\right], \\ &= \frac{\xi}{\omega(\xi+\mu)(\mu+\delta+d)}\frac{\Lambda(t'+\mu)}{\mu(\sigma+t'+\mu)+\lambda t'\sigma}\left[\omega\beta + \frac{\delta_{1n}\alpha_1\varphi}{\kappa} + \frac{\sigma}{t'+\mu}\left(\epsilon\omega + \frac{\delta_{1n}\alpha_2\varphi}{\kappa}\right)\right].\end{aligned} \tag{19}$$

It follows from Theorem 2 of [8] that the disease-free steady state is asymptotically stable in the case $\mathcal{R}_0 < 1$ and unstable if $\mathcal{R}_0 > 1$. In fact looking at the proof reveals that under the assumptions of that theorem the following stronger statements hold. In the case $\mathcal{R}_0 < 1$ all eigenvalues of the linearization at the disease-free steady state have negative real parts and in the case $\mathcal{R}_0 > 1$ the linearization has an eigenvalue with positive real part. This gives an indirect proof that the inequalities $\mathcal{A}_1\mathcal{A}_2 > \mathcal{A}_3$ and $\mathcal{A}_3 > 0$ of the last section hold.

In order to understand the effects of vaccination it is useful to write the basic reproductive ratio schematically in the form $\mathcal{R}_0 = A\left(\frac{B\sigma+C}{D\sigma+E}\right)$ where

$$A = \frac{\Lambda\xi}{\omega(\xi+\mu)(\mu+\delta+d)}, \tag{20}$$

$$B = \epsilon\omega + \frac{\delta_{1n}\alpha_2\varphi}{\kappa}, \tag{21}$$

$$C = (\mu+t')\left(\omega\beta + \frac{\delta_{1n}\alpha_1\varphi}{\kappa}\right), \tag{22}$$

$$D = \mu + \lambda t', \tag{23}$$

$$E = \mu(\mu+t'). \tag{24}$$

The sign of the derivative of $\mathcal{R}_0$ with respect to σ is equal to that of $BE - CD$. This last quantity is equal to

$$\omega(\mu+t')[(\epsilon-\beta)\mu - \lambda t'\beta] + \frac{\delta_{1n}\varphi}{\kappa}(\mu+t')[(\alpha_2-\alpha_1)\mu - \lambda t'\alpha_1]. \tag{25}$$

Under the assumptions made on the parameters it is negative and so we see that increasing the vaccination rate decreases $\mathcal{R}_0$, generalizing a result of [8].

3.2. Backward bifurcation analysis

The concept of a backward bifurcation is used in the literature on epidemiological models. It is defined in situations where a definition of the basic reproduction ratio $\mathcal{R}_0$ is available. In many models endemic steady states only exist in the case $\mathcal{R}_0 > 1$. We think of the direction of increasing $\mathcal{R}_0$ as the forward direction and that is where endemic steady states occur. There are, however, models where it happens that near $\mathcal{R}_0 = 1$ there are endemic steady states with $\mathcal{R}_0 < 1$, i.e. in the backward direction. The steady state bifurcates from the disease-free steady state as the parameter $\mathcal{R}_0$ is varied. A commonly occurring case is where there is a generic transcritical bifurcation for $\mathcal{R}_0 = 1$ and this covers both the forward and backward cases, these being distinguished by the sign of a parameter a. We call this case a generic backward bifurcation.

In our model the qualitative behaviour depends on a parameter which is a natural number n. For $n \neq 2$ we show that any generic transcritical bifurcation must be a forward bifurcation. Thus a generic backward bifurcation is impossible in that case. For $n = 2$ we show that generic backward bifurcations do occur for some values of the parameters.

When applying mathematical models to guide the practical management of epidemics a standard goal is to modify the situation (for instance by vaccinations or non-pharmaceutical interventions) so that the corresponding change in the parameters of the model is such that $\mathcal{R}_0$ becomes less than one. When a backward bifurcation is present this may not be enough to eradicate the infection since an endemic steady state can exist although $\mathcal{R}_0 < 1$. In that case $\mathcal{R}_0$ must be made less than $\mathcal{R}_1$ for a critical value $\mathcal{R}_1 < 1$. This suggests that the presence of backward bifurcations makes control of epidemics more difficult. However, as discussed in Section 9.2 of [23], this is not always the case. It sometimes happens that the subset of parameter space where the disease-free steady state is stable is larger for a model with backward bifurcation than for one without.

Consider the disease-free steady state $E^* = (S^*, 0, 0, V^*, R^*, 0)$ for the system (1)–(6). We choose β as the bifurcation parameter and denote its value at the bifurcation point where $\mathcal{R}_0 = 1$ by β^*. Then

$$\beta^* = \frac{(\xi+\mu)(\mu+\delta+d)}{\xi S^*} - \frac{\delta_{1n}\alpha_1\varphi}{\omega\kappa} - \left(\epsilon + \frac{\delta_{1n}\alpha_2\varphi}{\omega\kappa}\right)\frac{\sigma}{t'+\mu}, \tag{26}$$

where $S^* = \dfrac{\Lambda(t'+\mu)}{\mu(\sigma+t'+\mu)+\lambda t'\sigma}$. Note that for fixed values of the other parameters there is only a choice of β for which $\mathcal{R}_0 = 1$ if the right hand side of (26) is positive.

Following the ideas presented by [8], according to centre manifold theory, it is necessary to compute right and left eigenvectors of the Jacobian matrix evaluated at the disease-free steady state E^* and $\beta = \beta^*$. Consider a right eigenvector of the form $\underline{w} = (w_1, w_2, w_3, w_4, w_5, w_6)^T$. Thus the system leads to

$$-(\sigma+\mu)w_1 - \beta^* S^* w_3 + (1-\lambda)t' w_4 - \frac{\alpha_1\delta_{1n}}{\kappa} S^* w_6 = 0, \tag{27}$$

$$-(\xi+\mu)w_2 + (\beta^* S^* + \epsilon V^*)w_3 + \frac{\delta_{1n}}{\kappa}(\alpha_1 S^* + \alpha_2 V^*)w_6 = 0, \tag{28}$$

$$\xi w_2 - (\delta+d+\mu)w_3 = 0, \tag{29}$$

$$\sigma w_1 - \epsilon V^* w_3 - (t'+\mu)w_4 - \frac{\delta_{1n}\alpha_2}{\kappa} V^* w_6 = 0, \tag{30}$$

$$\delta\omega_3 + \lambda t' w_4 - \mu w_5 = 0, \tag{31}$$

$$\varphi w_3 - \omega w_6 = 0. \tag{32}$$

Using Eq. (29) and (32), we obtain

$$w_3 = \frac{\xi w_2}{\delta+d+\mu} \quad \text{and} \quad w_6 = \frac{\varphi\xi}{\omega(\delta+d+\mu)} w_2. \tag{33}$$

Using these in Eq. (28), we find

$$\left[\beta^* - \frac{(\delta+d+\mu)(\xi+\mu)}{\xi S^*} + \frac{\delta_{1n}\alpha_1\varphi}{\omega\kappa} + \left(\epsilon + \frac{\delta_{1n}\alpha_2\varphi}{\omega\kappa}\right)\frac{\sigma}{t'+\mu}\right] w_2 = 0, \tag{34}$$

Thus we see that (26) is a necessary condition for there to be a vector in the kernel with $w_2 \neq 0$. Note that if $w_2 > 0$ then w_3 and w_6 are positive, as they must be as a consequence of the general theory. Besides, using Eqs. (27) and (30), one obtains

$$-(\sigma+\mu)w_1 + (1-\lambda)t'w_4 = \left(\beta^* + \frac{\delta_{1n}\alpha_1\varphi}{\omega\kappa}\right)\frac{\xi S^*}{(\delta+d+\mu)}w_2, \tag{35}$$

$$\sigma w_1 - (t'+\mu)w_4 = \left(\epsilon + \frac{\delta_{1n}\alpha_2\varphi}{\omega\kappa}\right)\frac{\xi V^*}{(\delta+d+\mu)}w_2, \tag{36}$$

respectively. That leads to

$$w_1 = -\frac{\frac{\xi w_2}{\delta+d+\mu}\left[\left(\beta^* + \frac{\delta_{1n}\alpha_1\varphi}{\omega\kappa}\right)(t'+\mu)S^* + \left(\epsilon + \frac{\delta_{1n}\alpha_2\varphi}{\omega\kappa}\right)(1-\lambda)t'V^*\right]}{\mu(\sigma+t'+\mu)+\sigma\lambda t'} < 0, \tag{37}$$

for $\lambda \leq 1$ and

$$w_4 = -\frac{\frac{\xi w_2}{\delta+d+\mu}\left[\left(\beta^* + \frac{\delta_{1n}\alpha_1\varphi}{\omega\kappa}\right)\sigma S^* + \left(\epsilon + \frac{\delta_{1n}\alpha_2\varphi}{\omega\kappa}\right)(\sigma+\mu)V^*\right]}{\mu(\sigma+t'+\mu)+\sigma\lambda t'} < 0. \tag{38}$$

Furthermore using Eq. (31):

$$w_5 = \frac{\xi w_2}{\delta+d+\mu}\left[\delta - \lambda t'\frac{\left(\beta^* + \frac{\delta_{1n}\alpha_1\varphi}{\omega\kappa}\right)\sigma S^* + \left(\epsilon + \frac{\delta_{1n}\alpha_2\varphi}{\omega\kappa}\right)(\sigma+\mu)V^*}{\mu(\sigma+t'+\mu)+\sigma\lambda t'}\right]. \tag{39}$$

In a similar manner, a left eigenvector can be written in the form $\underline{v} = (v_1, v_2, v_3, v_4, v_5, v_6)$ for which

$$v_5 = 0, \tag{40}$$

$$-(\sigma+\mu)v_1 + \sigma v_4 = 0, \tag{41}$$

$$-(\xi+\mu)v_2 + \xi v_3 = 0, \tag{42}$$

$$-\beta^* S^* v_1 + (\beta^* S^* + \epsilon V^*)v_2 - (\delta+d+\mu)v_3 - \epsilon V^* v_4 + \varphi v_6 = 0, \tag{43}$$

$$(1-\lambda)t'v_1 - (t'+\mu)v_4 = 0, \tag{44}$$

$$-\frac{\delta_{1n}\alpha_1}{\kappa}S^* v_1 + \frac{1}{\kappa}(\delta_{1n}\alpha_1 S^* + \delta_{1n}\alpha_2 V^*)v_2 - \frac{\delta_{1n}\alpha_2}{\kappa}V^* v_4 - \omega v_6 = 0. \tag{45}$$

Using (41) and (44), we find

$$\left(\sigma\lambda t' + \mu(\sigma+\mu+t')\right)v_4 = 0, \tag{46}$$

leading to $v_4 = 0$ and thus $v_1 = 0$. In addition, from Eqs. (42) and (45), we obtain

$$v_3 = \left(1 + \frac{\mu}{\xi}\right)v_2, \quad \text{and} \quad v_6 = \frac{\delta_{1n}}{\kappa\omega}\left(\alpha_1 S^* + \alpha_2 V^*\right)v_2. \tag{47}$$

Thus the left eigenvector becomes

$$\underline{v} = \left(0, v_2, \left(1 + \frac{\mu}{\xi}\right)v_2, 0, 0, \frac{\delta_{1n}}{\kappa\omega}(\alpha_1 S^* + \alpha_2 V^*)v_2\right), \tag{48}$$

and we find

$$\underline{w}\cdot\underline{v} = \left(1 + \frac{\xi+\mu}{\delta+d+\mu} + \frac{\delta_{1n}\varphi\xi}{\kappa\omega^2(\delta+d+\mu)}\right)w_2 v_2 > 0. \tag{49}$$

Let a be the bifurcation coefficient introduced in [8]. Considering the model (1)–(6) in the form $\dot{x}_i = f_i(x_i)$, $i = \{1,2,3,4,5,6\}$, it is given by

$$a = \sum_{k,i,j=1}^{6} v_k w_i w_j \frac{\partial^2 f_k}{\partial x_i \partial x_j}(0,0). \tag{50}$$

Using Eqs. (48) and (50)

$$a = v_2 \sum_{i,j=1}^{6} w_i w_j \frac{\partial^2 f_2}{\partial x_i \partial x_j} + \left(1 + \frac{\mu}{\xi}\right)v_2 \sum_{i,j=1}^{6} w_i w_j \frac{\partial^2 f_3}{\partial x_i \partial x_j}$$

$$+\frac{\delta_{1n}(\alpha_1 x_1^* + \alpha_2 x_4^*)}{\kappa\omega} v_2 \sum_{i,j=1}^{6} w_i w_j \frac{\partial^2 f_6}{\partial x_i \partial x_j},$$

where

$$f_2 = \beta^* x_1 x_3 + \epsilon x_3 x_4 - \xi x_2 - \mu x_2 + \alpha_1 x_1 g(x_6, \kappa) + \alpha_2 x_4 g(x_6, \kappa),$$
$$f_3 = \xi x_2 - (\delta + d + \mu) x_3,$$
$$f_6 = \varphi x_3 - \omega x_6.$$

Note that $\frac{\partial g}{\partial C}(0,\kappa) = \kappa^{-1}$ for $n = 1$ and zero otherwise. $\frac{\partial^2 g}{\partial C^2}(0,\kappa)$ is equal to $-2\kappa^{-2}$ for $n = 1$, $2\kappa^{-1}$ for $n = 2$ and zero otherwise. Since second derivatives of f_3 and f_6 with respect to x_i, $i = \{1,2,3,4,5,6\}$ are always zero;

$$a = 2v_2 \left[w_1 w_3 \beta^* + w_3 w_4 \epsilon \right.$$
$$\left. + (\alpha_1 w_1 + \alpha_2 w_4) w_6 \frac{\partial g}{\partial C}(0,\kappa) + (\alpha_1 x_1^* + \alpha_2 x_4^*) w_6^2 \frac{\partial^2 g}{\partial C^2}(0,\kappa) \right]. \tag{51}$$

We want to determine the sign of a and since $v_2 > 0$ this is the same as that of the expression in square brackets. The first two summands are negative. Now $(w_1 + w_4)w_6 < 0$ and $w_6^2 > 0$. Hence in the case $n = 1$ we see that all summands are negative and hence $a < 0$. It follows that in that case the conditions for a backward bifurcation given in [8] cannot be satisfied. The same conclusion is obtained in the case $n \geq 3$. In the exceptional case $n = 2$ the last summand is positive and so we investigate further whether a backward bifurcation can take place in that case. In the notation of [8] we have

$$b = \sum_{k,i=1}^{6} w_k w_i \frac{\partial^2 f_k}{\partial x_i \partial \beta}(0,0). \tag{52}$$

Since only f_1 and f_2 involve the parameter β, derivatives with respect to x_1 and x_3 are non-zero. Here

$$b = w_3 x_1^* (w_2 - w_1) > 0. \tag{53}$$

It follows from [8] that there is a backward bifurcation precisely when the right hand side of (26) is positive and

$$2(\alpha_1 S^* + \alpha_2 V^*) w_6^2 \kappa^{-1} > -w_3(w_1 \beta^* + w_4 \epsilon). \tag{54}$$

Note that in the case $n > 1$ the expression for β^* simplifies to

$$\beta^* = \frac{(\xi + \mu)(\mu + \delta + d)\left[\mu(\sigma + t' + \mu) + \lambda t' \sigma\right] - \Lambda \xi \epsilon \sigma}{\Lambda \xi (t' + \mu)}. \tag{55}$$

Do there exist values of the parameters for which these conditions are satisfied? To investigate this we substitute the expressions for w_6, w_3, w_1 and w_4 into (54). The result is

$$2(\alpha_1 S^* + \alpha_2 V^*) \frac{\varphi^2}{\omega^2 \kappa}$$
$$> \frac{\Lambda[(\beta^*)^2 (t' + \mu)^2 + \beta^* \epsilon((2 - \lambda)t' + \mu)\sigma + \epsilon^2 t' \sigma(\sigma + \mu)]}{[\mu(\sigma + t' + \mu) + \sigma \lambda t']^2}. \tag{56}$$

Using the expressions for S^* and V^* this can be simplified to

$$2(\alpha_1 (t' + \mu) + \alpha_2 \sigma) \frac{\varphi^2}{\omega^2 \kappa}$$
$$> \frac{[(\beta^*)^2 (t' + \mu)^2 + \beta^* \epsilon((2 - \lambda)t' + \mu)\sigma + \epsilon^2 t' \sigma(\sigma + \mu)]}{\mu(\sigma + t' + \mu) + \sigma \lambda t'}. \tag{57}$$

Thus it is clear that if α_1 or α_2 is made large enough while the other parameters are kept fixed then there is a backward bifurcation. It is important to note that the parameters given for the case $n = 2$ in Table 3 satisfy the conditions for a backward bifurcation in (57). These results with now be summed up.

Theorem 1. *If $n = 2$ and the parameters in the system (1)–(6) satisfy the inequality (57) with the quantity β^* defined by (55) being positive then the parameter a of [8] is positive and a generic backward bifurcation occurs. There exist parameters for which these conditions are satisfied. If $n \neq 2$ the condition $a > 0$ is never satisfied.*

Note that if $\alpha_1 = \alpha_2 = 0$ but $t' \neq 0$ no backward bifurcation occurs. This means that in the context of our model imperfect vaccination alone does not give rise to a backward bifurcation. Infection from the environment is required.

The centre manifold at the bifurcation point is one-dimensional. Since $v_3 > 0$ we can use I as a parameter on the centre manifold. The restriction of the dynamical system to the centre manifold is of the form $\dot{I} = f(I, \beta)$, where we have suppressed the dependence on the parameters other than β in the notation. With this notation the sign of a is equal to that of $\frac{\partial^2 f}{\partial I^2}$ while that of b is equal to that of $\frac{\partial^2 f}{\partial I \partial \beta}$. We have $f(0,\beta) = 0$ for all β. Moreover there is a curve $c(\beta)$ of steady states with $c(\beta^*) = 0$. The sign of $c'(\beta^*)$ is equal to that of a.

4. Endemic steady states

In this section we consider endemic steady states, i.e. those where all the unknowns are positive. It follows from (4) that at a steady state $V = \frac{\sigma}{\epsilon I+(t'+\mu)+\alpha_2 g} S$. Substituting this into (1) gives

$$S = \frac{\Lambda}{\beta I + \sigma + \alpha_1 g + \mu}\left[1 - \frac{(1-\lambda)t'\sigma}{(\beta I + \sigma + \alpha_1 g + \mu)(\epsilon I + (t'+\mu) + \alpha_2\ g)}\right]^{-1}$$
$$= \frac{\Lambda(\epsilon I + (t'+\mu) + \alpha_2\ g)}{(\beta I + \sigma + \alpha_1 g + \mu)(\epsilon I + (t'+\mu) + \alpha_2\ g) - (1-\lambda)t'\sigma}, \tag{58}$$

where $g = g(C, \kappa)$. Note also that due to (6) we have $C = \frac{\varphi}{\omega} I$ and that due to (3) we have $E = \frac{(\delta+d+\mu)}{\xi} I$. These relations allow S, E, V and C to be expressed in terms of I. Thus substituting them into (2) gives an equation for I alone. Each summand contains a factor I and for an endemic steady state this can be cancelled. There remains

$$0 = \beta S + \epsilon V - \frac{(\xi+\mu)(\delta+d+\mu)}{\xi} + (\alpha_1 S + \alpha_2 V)\frac{(\varphi/\omega)^n I^{n-1}}{(\varphi/\omega)^n I^n + \kappa} \tag{59}$$

Denote the expression in the denominator of (58) by Z. Multiplying (59) by $Z[(\varphi/\omega)^n I^n + \kappa]$ gives a polynomial equation $p(I) = 0$ for I, see Appendix for details. Endemic steady states are in one to one correspondence with positive roots of p.

Since we are most interested in the case with backward bifurcations we now restrict to the case $n = 2$, where there are considerable simplifications in these formulae. It is clear that $p(I) \to -\infty$ as $I \to \infty$. Moreover $p(0)$ is equal to a positive factor times

$$\beta S^* + \epsilon V^* - \frac{(\xi+\mu)(\delta+d+\mu)}{\xi}. \tag{60}$$

We see that the sign of $p(0)$ is the same as that of $\mathcal{R}_0 - 1$. As β increases through β^* the sign of $p(0)$ changes from negative to positive. When $p'(0) \neq 0$ we have a generic transcritical bifurcation (cf. [24], Section 3.1). The sign of $p'(0)$ is the same as that of $c'(\beta^*)$ in the discussion of the centre manifold in the previous section. If $p'(0) < 0$ then for β slightly greater than β^* there exists a positive root of p close to zero and hence a positive steady state close to the disease free steady state. This corresponds to a forward bifurcation. If, on the other hand, $p'(0) > 0$ then for β slightly less than β^* there exists a positive root of p close to zero and hence a positive steady state close to the disease free steady state. This corresponds to a backward bifurcation. In this case p is positive for I slightly larger than its value I_1 at that steady state. By the intermediate value theorem there must exist some $I_2 > I_1$ with $p(I_2) = 0$ and hence a second positive steady state. The direction of the flow on the centre manifold shows that the steady state with $I = I_1$ is unstable. The stability of the steady state with $I = I_2$ cannot be determined by the arguments we have presented. A simulation whose results are shown in Fig. 7 indicates that in fact the latter steady state is stable and that it does not come close to the disease-free steady state in the parameter range considered.

5. Simulations

In a broad context, the process of mathematical modelling and data fitting revolves around formulating mathematical models that describe real-world phenomena and then adjusting the parameters of these models to best match observed data. Therefore, the aim is to capture the underlying relationships and behaviour of the system being studied and use the available data to validate the model. In our study, we ensure the validation of the mathematical model of the COVID-19 outbreak by using the data fitting of the model regarding the observed data. However, the available data is scarce (only the actual data for infectious and vaccinated people are almost certain). Vaccination is globally considered to be the most effective solution for infectious diseases such as the recent COVID-19 outbreak. In this section, as an example, model results and observed data for the vaccinated class are compared for COVID-19 scenarios in Turkey. Some of the realistic parameters are taken from the literature, see the related references in Table 3 for a detailed discussion of parameter choices. The remaining seven parameters are estimated, by fitting the vaccinated compartment generated from the system (1)–(6) to the observed number of COVID-19 vaccinated individuals using standard model-fitting procedures.

The least squares method is the process of finding the best-fitting curve or line of best fit for a set of data points by reducing the sum of the squares of the offsets (residual part) of the points from the curve. The vector consisting of seven parameters $p = (\beta, \epsilon, \alpha_1, \alpha_2, \xi, \delta, \sigma)$ can be estimated via *parameter estimation*. In this context, the model given by (1)–(6) is evaluated by considering a non-linear least squares problem with positive constraints, where the best fitting curve can be found for a small data set of vaccinated class by minimizing the sum of squares of the deviations of data points from the plotted graph [9,25]. This may be described as

$$S(p) = \sum \left(V_i - \mathcal{F}(x_i, p)\right)^2, \tag{61}$$

where V_i represents the data set and $\mathcal{F}(x_i, p)$ denotes the model result with for a vector of unknowns p. To minimize the function $S(p)$, the non-linear least square minimization routine *lsqcurvefit* of MATLAB is used [26]. Parameters obtained from this approach are given in Table 3. Besides MATLAB's standard *ode45* solver [26] is applied for numerical integration of the system (1)–(6) with suitable initial conditions provided in the text.

Numerical simulations of the model (1)–(6) can be shown with the parameters given in Table 3 for $n = 1$. An example data set of vaccinated people during the COVID−19 outbreak in Turkey is taken from the World Health Organisation. In Fig. 2, the results

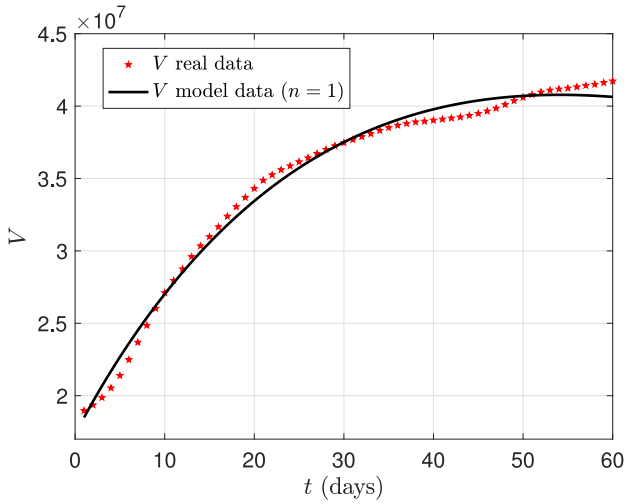

Fig. 2. Vaccination component for the model for the case with $n = 1$ is compared with real data for the period of June 10, 2021 and August 8, 2021. Parameters are given in Table 3. Initial conditions are chosen as $S_0 = 61098000, V_0 = 18500000, E_0 = 2200000, R_0 = 2000, C_0 = 20000$. The black line denotes the model result and the red stars represent daily vaccinated cases.

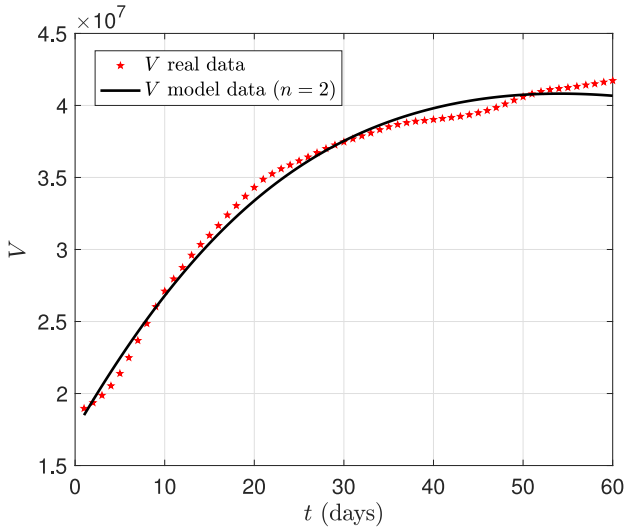

Fig. 3. Vaccination component for the model for the case with $n = 2$ is compared with real data for the period of June 10, 2021 and August 8, 2021. Parameters are given in Table 3. Initial conditions are chosen as $S_0 = 61098000, V_0 = 18500000, E_0 = 2200000, R_0 = 2000, C_0 = 20000$. The black line denotes the model result and the red stars represent daily vaccinated cases.

are shown for model (1)–(6) with $n = 1$ fitted to the data of individuals vaccinated between June 10, 2021 and August 8, 2021. The total population is taken 83 million [27].

In Fig. 3, success of parameter estimation is again demonstrated. Here numerical simulations of the model (1)–(6) with $n = 2$ is shown with the parameters given in Table 3 and the resulting outcome is compared with the data set of vaccinated people between June 10, 2021 and August 8, 2021. As seen, in Figs. 2 and 3, the black curve corresponding to the model becomes flattened after around day 40 and this agrees with the real data, where the real number of vaccinated people rapidly increases from 18 967 237 to 41 726 338 and it is smoothed roughly about July 20.

6. Sensitivity analysis

Since varying the parameters may have a significant impact on the model output, one can perform a sensitivity analysis of the dynamical model to determine which model parameters are more influential for the dynamics. The parameters associated with the basic reproduction ratio $\mathcal{R}_0$ have particular importance for the robustness of the model. In this context, the aim of the sensitivity analysis is to identify the most substantial parameter in the model for disease transmission.

Table 3
Estimated parameters of the model.

Parameters	Value ($n = 1$)	Value ($n = 2$)	Unit	Source
Λ	3032	3032	day^{-1}	Assumed based on [10,18,19]
β	1.0257×10^{-8}	1.004×10^{-8}	day^{-1}	Estimated
μ	3.653×10^{-5}	3.653×10^{-5}	day^{-1}	Assumed based on [9,10,27]
ϵ	1×10^{-8}	1×10^{-8}	day^{-1}	Estimated
ι'	0.0055	0.0055	day^{-1}	Assumed based on [12]
λ	0.8	0.8	day^{-1}	Assumed based on [12,20,21]
d	0.1	0.1	day^{-1}	Assumed based on [9,22]
α_1	0.00041	0.0001	day^{-1}	Estimated
α_2	0.00031	0.0001	day^{-1}	Estimated
ω	5	5	day^{-1}	[9]
φ	2	2	day^{-1}	[9]
κ	20 000	20 000	copies/day	Assumed based on [9,28]
ξ	0.01004	0.01133	day^{-1}	Estimated
δ	0.19999	0.2	day^{-1}	Estimated
σ	0.02136	0.02126	day^{-1}	Estimated

Table 4
Sensitivity indices of basic reproduction ratio of model (1)–(6), considering at the baseline parameters provided in Table 3. number for $n = 1$ and $n = 2$.

Parameters	Index ($n = 1$)	Index ($n = 2$)
β	0.1276764	0.2089141
ϵ	0.4754643	0.7910858
$\iota\prime$	−0.7636042	−0.7843018
λ	−0.9897355	−0.9897256
d	−0.3333038	−0.3332927
α_1	0.1020714	0
α_2	0.2947878	0
ξ	0.0036252	0.0032138
δ	−0.6665743	−0.6665855
σ	−0.2276182	−0.2067744

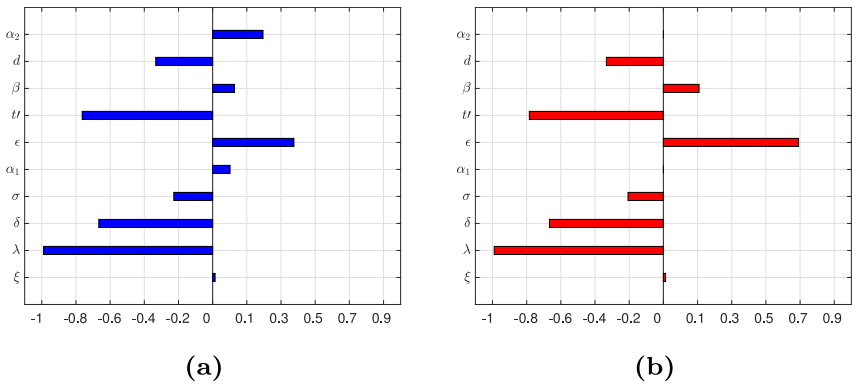

Fig. 4. Sensitivity indices based on basic reproduction ratio $\mathcal{R}_0$ with respect to various parameters given for Cases $n = 1$ (a) and $n = 2$ (b) in the model (1)–(6) for Turkey. Parameter values given in Table 3 are considered for both cases.

Following the ideas presented in [29,30], the sensitivity analysis can be performed based on the basic reproduction ratio as

$$S_i^{\mathcal{P}} = \frac{\mathcal{P}}{\mathcal{R}_0} \frac{\partial \mathcal{R}_0}{\partial \mathcal{P}}, \tag{62}$$

where $\mathcal{P}$ represents a generic parameter in the model (1)–(6).

The sensitivity indices of the system parameters in Table 3 are demonstrated in 4, and also in Figs. 4(a) for $n = 1$ and 4(b) for $n = 2$.

As seen from Table 4 and Fig. 4, the model (1)–(6) is highly sensitive to the parameters λ, ι' and δ. Thus it can be concluded that an increase in these parameters diminishes the basic reproduction ratio $\mathcal{R}_0$ for both $n = 1$ and $n = 2$. The significance of some parameters may be different between Case 1 and Case 2. For example, although the increase in the parameter ϵ, i.e. the rate at which a vaccinated individual becomes exposed after being in contact with an infected individual, leads to an essential stimulus for the basic reproduction ratio for Case 2, yet it has a much smaller impact on the $\mathcal{R}_0$ for the case $n = 1$.

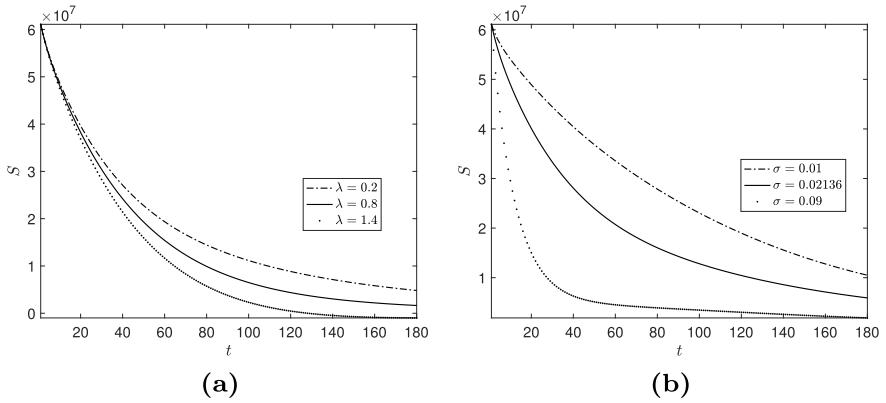

Fig. 5. Plots for susceptible population compartment for different values of vaccine efficiency $\lambda = 0.2, 0.8, 1.4$ and for different values of vaccination rate of susceptible individuals after the first shot, $\sigma = 0.01, 0.02136, 0.09$ with $n = 1$.

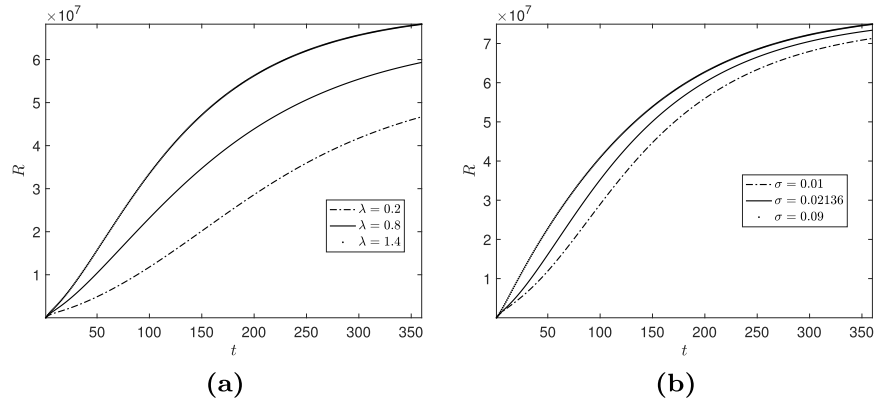

Fig. 6. Plots for recovery compartment for different values of vaccine efficiency $\lambda = 0.2, 0.8, 1.4$; and for different values of vaccination rate of susceptible individuals after the first shot, $\sigma = 0.01, 0.02136, 0.09$ with $n = 1$.

Since the aim of our work is to further broaden the current knowledge of the modelling of recent COVID-19 outbreak with vaccination, we focus on the role of two parameters regarding vaccination in the model. In Fig. 5, time simulations of the Susceptible compartment over a period of 180 days are presented for various rates of $\lambda = 0.2, 0.8, 1, 4$ (a) and $\sigma = 0.01, 0.02136, 0.09$ (b), respectively denotes the efficiency of the vaccine and the vaccination rate of susceptible (after the first shot). As is seen from Fig. 5 (a,b), with the increase in λ and σ, susceptible individuals diminish at an earlier time and enter the vaccinated class.

Fig. 6 demonstrates time simulations of the recovered class over a period of 360 days for various rates of $\lambda = 0.2, 0.8, 1, 4$ and $\sigma = 0.01, 0.02136, 0.09$.

Fig. 7 shows that the system (1)–(6) undergoes a backward bifurcation at $R_0 = 1$ ($\beta = 1.656 \times 10^{-6}$) using the parameters given in Table 3. Here, there is a region where a stable endemic equilibrium (EE) co-exists with a stable disease-free equilibrium (DFE) when $R_0 < 1$. This situation may result in important implications for public health, as it indicates the necessity of the basic reproduction number being less than unity, but not sufficient to wipe out the disease [23].

7. Conclusion and outlook

In this paper a model for an epidemic with a partially effective vaccination and infection by virus in the environment is studied. Two different implementations of the idea of a partially effective vaccination are included and which of these is chosen does not seem to have an essential influence on the qualitative behaviour of the solutions. In modelling infections coming from the environment we used a phenomenological model for the force of infection containing an integer $n \geq 1$ as a parameter. We discovered that the choice $n = 2$ leads to the occurrence of backward bifurcations while other choices of n do not. Thus here there is a major qualitative difference. On the other hand, fitting to real data for COVID-19 in Turkey showed that both the cases $n = 1$ and $n = 2$ worked and there was no clear indication that one of these choices was better than the other according to that criterion.

In the case $n = 2$ it was shown that for certain values of the parameters there exists an endemic steady state although $\mathcal{R}_0 < 1$. It was also shown that in this situation there exist more than one endemic steady state. At least one of the positive steady states is unstable. This confirms rigorously that certain aspects of the usual picture of a backward bifurcation are present in this model. An

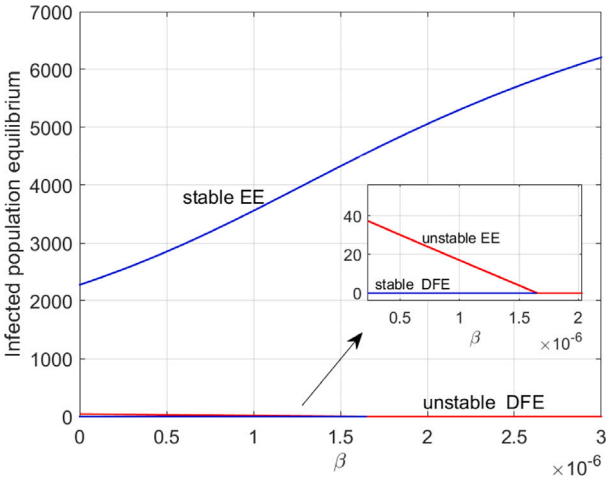

Fig. 7. Backward bifurcation diagram for the parametric values given in Table 3 for $n = 2$. The red and blue lines denote unstable and stable equilibrium points, respectively.

aspect of this picture which was not reproduced here is that the other positive steady state should be stable. It would be desirable to prove a stability statement of this kind analytically.

An outstanding challenge is to provide a mechanistic derivation of the response function for infections coming from the environment. If this could be done then it would help to decide which value of n in the Ansatz we used is more appropriate for modelling a given disease or whether, indeed, a different type of function would give better results.

Funding

Aytül Gökçe was partially supported by a grant from the Niels Hendrik Abel Board, Norway.

CRediT authorship contribution statement

Aytül Gökçe: Conceptualization, Methodology, Visualization, Software, Writing – original draft. **Burcu Gürbüz:** Conceptualization, Investigation, Data curation, Validation, Writing – original draft. **Alan D. Rendall:** Supervision, Conceptualization, Validation, Writing – review & editing.

Declaration of competing interest

The authors declare that they have no known competing financial interests or personal relationships that could have appeared to influence the work reported in this paper.

Data availability

Data available on reasonable request from the authors.

Appendix

Denote the expression in the denominator of (58) by Z. Multiplying (59) by $Z[(\varphi/\omega)^n I^n + \kappa]$ gives a sixth order polynomial equation $p(I) = 0$ for I as

$$p(I) = a_0 I^6 + a_1 I^5 + a_2 I^4 + a_3 I^3 + a_4 I^2 + a_5 I + a_6, \tag{63}$$

where

$$a_0 = -\nu b_1,$$
$$a_1 = \beta \Lambda \epsilon \left(\frac{\varphi}{\omega}\right)^4 - \nu b_2,$$
$$a_2 = \Lambda \left[\beta \left(t' + \mu + \alpha_2\right) + \epsilon \left(\sigma + \alpha_1\right)\right] \left(\frac{\varphi}{\omega}\right)^4 - \nu b_3,$$
$$a_3 = \Lambda \left[\alpha_1 (t' + \mu + \alpha_2) + \alpha_2 \sigma\right] \left(\frac{\varphi}{\omega}\right)^4 + 2\beta \Lambda \epsilon \kappa \left(\frac{\varphi}{\omega}\right)^2 - \nu b_4,$$

$$a_4 = \Lambda\kappa\left[2(\beta(t'+\mu)+\epsilon\sigma)+\beta\alpha_2+\epsilon\alpha_1\right]\left(\frac{\varphi}{\omega}\right)^2 - \nu b_5,$$
$$a_5 = \beta\Lambda\epsilon\kappa^2 + \Lambda\kappa\left(\alpha_1(t'+\mu)+\alpha_2\sigma\right)\left(\frac{\varphi}{\omega}\right)^2 - \nu b_6,$$
$$a_6 = \Lambda\kappa^2\left(\beta(t'+\mu)+\epsilon\sigma\right) - \nu b_7,$$

Here $\nu = (\xi+\mu)(\delta+d+\mu)/\xi$ and

$$b_1 = \beta\epsilon\left(\frac{\varphi}{\omega}\right)^4,$$
$$b_2 = \left[\beta(t'+\mu+\alpha_2)+\epsilon(\sigma+\mu+\epsilon)\right]\left(\frac{\varphi}{\omega}\right)^4,$$
$$b_3 = \left[(t'+\mu+\alpha_2)(\sigma+\mu+\alpha_1)-(1-\lambda)t'\sigma\right]\left(\frac{\varphi}{\omega}\right)^4 + 2\beta\kappa\epsilon\left(\frac{\varphi}{\omega}\right)^2,$$
$$b_4 = \kappa\left[2\beta(t'+\mu)+2\epsilon(\sigma+\mu)+\beta\alpha_2+\epsilon\alpha_1\right]\left(\frac{\varphi}{\omega}\right)^2,$$
$$b_5 = \kappa\left[(\sigma+\mu)(t'+\mu+\alpha_2)+(t'+\mu)(\sigma+\mu+\alpha_1)-2(1-\lambda)t'\sigma\right]\left(\frac{\varphi}{\omega}\right)^2 + \beta\epsilon\kappa^2,$$
$$b_6 = \kappa^2\left[\beta(t'+\mu)+\epsilon(\sigma+\mu)\right],$$
$$b_7 = \kappa^2\left[(\sigma+\mu)(t'+\mu)-(1-\lambda)t'\sigma\right].$$

Endemic steady states are in one to one correspondence with positive roots of p in Eq. (63).

References

[1] R. Ross, An application of the theory of probability to the theory of a priori pathometry. Part I, Proc. R. Soc. Lond. Ser. A 92 (1916) 204–230.
[2] R. Ross, H.P. Hudson, An application of the theory of probability to the theory of a priori pathometry. Part II, Proc. R. Soc. Lond. Ser. A 93 (1917) 212–225.
[3] R. Ross, H.P. Hudson, An application of the theory of probability to the theory of a priori pathometry. Part III, Proc. R. Soc. Lond. Ser. A 93 (1917) 225–240.
[4] J. Zhao, J.E. Eisenberg, I.H. Spicknall, S. Li, J.S. Koopman, Model analysis of fomite mediated influenza transmission, PloS ONE 7 (2012) e51984.
[5] C.J. Sunyok, L. Fox, H. Ritchie, C. Lanzas, S. Lenhart, Mathematically modelling the effect of touch frequency on the environmental transmission of *Clostridioides difficile* in healthcare settings, Math. Biosci. 340 (2021) 108666.
[6] G. Anderson, R.J. Reiter, Melatonin: Roles in influenza, COVID-19, and other viral infections, Rev. Med. Virol. 30 (2020) e2019.
[7] S.W. Park, D.M. Cornforth, J. Dushoff, J.S. Weitz, The time scale of asymptomatic transmission affects estimates of epidemic potential in the COVID-19 outbreak, Epidemics 31 (2020) 100392.
[8] P. Van den Driessche, J. Watmough, Reproduction numbers and sub-threshold endemic equilibria for compartmental models of disease transmission, Math. Biosci. 180 (1–2) (2002) 29–48.
[9] H. Bulut, M. Gölgeli, F.M. Atay, Modelling personal cautiousness during the COVID-19 pandemic: a case study for Turkey and Italy, Nonlinear Dyn. 105 (1) (2021) 957–969.
[10] A.B. Gumel, C.C. McCluskey, J. Watmough, An SVEIR model for assessing potential impact of an imperfect anti-SARS vaccine, Math. Biosci. Eng. 3 (2006) 485–512.
[11] M. Martcheva, Methods for deriving necessary and sufficient conditions for backward bifurcation, J. Biol. Dyn. 13 (2019) 538–566.
[12] M. Angeli, G. Neofotistos, M. Mattheakis, E. Kaxiras, Modeling the effect of the vaccination campaign on the COVID-19 pandemic, Chaos Solitons Fractals 154 (2022) 111621.
[13] O. Diekmann, J.A.P. Heesterbeek, Mathematical Epidemiology of Infectious Diseases, Wiley, 2000.
[14] J.H.P. Dawes, M. Souza, A derivation of Holling's type I, II and III functional responses in predator–prey systems, J. Theoret. Biol. 327 (2013) 11–22.
[15] C.S. Holling, Some characteristics of simple types of predation and parasitism, Can. Entomol. 91 (7) (1959) 385–398.
[16] K. Dietz, in: R. Anderson, R. May (Eds.), Overall Population Patterns in the Transmission Cycle of Infectious Disease Cycles, in Population Biology of Infectious Diseases, Springer, 1982.
[17] A.D. Rendall, Mathematics of the NFAT signalling pathway, SIAM J. Appl. Dyn. Syst. 11 (2012) 988–1006.
[18] V.P. Bajiya, S. Bugalia, J.P. Tripathi, Mathematical modeling of COVID-19: Impact of non-pharmaceutical interventions in India, Chaos 30 (11) (2020) 113143.
[19] S.M. Garba, M.A. Safi, A.B. Gumel, Cross-immunity-induced backward bifurcation for a model of transmission dynamics of two strains of influenza, Nonlinear Anal. RWA 14 (3) (2013) 1384–1403.
[20] L.R. Baden, H.M. El Sahly, B. Essink, K. Kotloff, S. Frey, R. Novak, D. Diemert, S.A. Spector, N. Rouphael, C.B. Creech, et al., Efficacy and safety of the mRNA-1273 SARS-CoV-2 vaccine, N. Engl. J. Med. 384 (5) (2021) 403–416.
[21] F.P. Polack, S.J. Thomas, N. Kitchin, J. Absalon, A. Gurtman, S. Lockhart, J.L. Perez, G. Pérez Marc, E.D. Moreira, C. Zerbini, et al., Safety and efficacy of the BNT162b2 mRNA COVID-19 vaccine, N. Engl. J. Med. 383 (27) (2020) 2603–2615.
[22] H. Ritchie, E. Ortiz-Ospina, D. Beltekian, E. Mathieu, J. Hasell, B. Macdonald, C. Giattino, M. Roser, A. Breck Yunits, D. Gavrilov, et al., Mortality Risk of COVID-19, Our World in Data [Internet], 2020, [cited 5 May 2020]. Available: https://ourworldindata.org/mortality-risk-covid#the-case-fatality-rate.
[23] Z.S. Kifle, L.L. Obsu, Co-dynamics of COVID-19 and TB with COVID-19 vaccination and exogenous reinfection for TB: An optimal control application, Infect. Dis. Model. (2023).
[24] S. Wiggins, Introduction To Applied Nonlinear Dynamical Systems and Chaos, Springer, 1990.
[25] T.F. Coleman, Y. Li, An interior trust region approach for nonlinear minimization subject to bounds, SIAM J. Optim. 6 (2) (1996) 418–445.
[26] The MathWorks Inc., MATLAB version: 9.13.0 (R2020b), 2020, URL https://www.mathworks.com.
[27] Türkiye İstatistik Kurumu (TUİK), https://www.tuik.gov.tr/.
[28] C. Drosten, L.-L. Chiu, M. Panning, H.N. Leong, W. Preiser, J.S. Tam, S. Günther, S. Kramme, P. Emmerich, W.L. Ng, et al., Evaluation of advanced reverse transcription-PCR assays and an alternative PCR target region for detection of severe acute respiratory syndrome-associated coronavirus, J. Clin. Microbiol. 42 (5) (2004) 2043–2047.
[29] N. Chitnis, J.M. Hyman, J.M. Cushing, Determining important parameters in the spread of malaria through the sensitivity analysis of a mathematical model, Bull. Math. Biol. 70 (2008) 1272–1296.
[30] M. Martcheva, An Introduction To Mathematical Epidemiology, Springer, 2015.